MOLECULAR AND CELLULAR BIOLOGY, Mar. 2006, p. 1700–1709 Vol. 26, No. 5
0270-7306/06/$08.00+0 doi:10.1128/MCB.26.5.1700–1709.2006

Targeted Disruption of Fibulin-4 Abolishes Elastogenesis and Causes Perinatal Lethality in Mice

Precious J. McLaughlin,[1]† Qiuyun Chen,[1]† Masahito Horiguchi,[2] Barry C. Starcher,[3] J. Brett Stanton,[1] Thomas J. Broekelmann,[4] Alan D. Marmorstein,[1,5] Brian McKay,[1,6] Robert Mecham,[4] Tomoyuki Nakamura,[2] and Lihua Y. Marmorstein[1,6,7]*

Department of Ophthalmology and Vision Science,[1] Optical Sciences Center,[5] Department of Cell Biology and Anatomy,[6] and Department of Physiology,[7] University of Arizona, Tucson, Arizona; Horizontal Medical Research Organization, Kyoto University School of Medicine, Kyoto, Japan[2]; Department of Biochemistry, University of Texas Health Center at Tyler, Texas[3]; and Department of Cell Biology and Physiology, Washington University School of Medicine, St. Louis, Missouri[4]

Received 20 October 2005/Returned for modification 27 November 2005/Accepted 5 December 2005

Elastic fibers provide tissues with elasticity which is critical to the function of arteries, lungs, skin, and other dynamic organs. Loss of elasticity is a major contributing factor in aging and diseases. However, the mechanism of elastic fiber development and assembly is poorly understood. Here, we show that lack of fibulin-4, an extracellular matrix molecule, abolishes elastogenesis. *fibulin-4*$^{-/-}$ mice generated by gene targeting exhibited severe lung and vascular defects including emphysema, artery tortuosity, irregularity, aneurysm, rupture, and resulting hemorrhages. All the homozygous mice died perinatally. The earliest abnormality noted was a uniformly narrowing of the descending aorta in *fibulin-4*$^{-/-}$ embryos at embryonic day 12.5 (E12.5). Aorta tortuosity and irregularity became noticeable at E15.5. Histological analysis demonstrated that *fibulin-4*$^{-/-}$ mice do not develop intact elastic fibers but contain irregular elastin aggregates. Electron microscopy revealed that the elastin aggregates are highly unusual in that they contain evenly distributed rod-like filaments, in contrast to the amorphous appearance of normal elastic fibers. Desmosine analysis indicated that elastin cross-links in *fibulin-4*$^{-/-}$ tissues were largely diminished. However, expression of tropoelastin or lysyl oxidase mRNA was unaffected in *fibulin-4*$^{-/-}$ mice. In addition, fibulin-4 strongly interacts with tropoelastin and colocalizes with elastic fibers in culture. These results demonstrate that fibulin-4 plays an irreplaceable role in elastogenesis.

Elastic fibers with morphologically distinct architectures are present in the extracellular matrix (ECM) to accommodate elastic requirements and mechanical stresses imposed on different tissues. They are particularly abundant in elastic tissues such as large blood vessels, lung, and skin. Loss of elasticity is a major contributing factor in aging and a myriad of pathological conditions including emphysema, artery diseases, and cutis laxa (39, 41, 44). Elastic fibers undergo irreversible structural and compositional changes with age and in some pathological conditions (41). Regardless of morphology, all elastic fibers consist of cross-linked elastin, fibrillin-rich microfibrils, and several associated molecules (23, 37, 38, 46). Elastin endows the fiber with the characteristic property of elastic recoil. It is chemically inert, extremely hydrophobic, and insoluble under most conditions. Monomeric elastin, called tropoelastin, is secreted from the cell as a soluble protein. Isolated and purified tropoelastin has been shown to exhibit a great tendency to aggregate (coacervation) in physiological solution and at temperatures in the physiological range, giving rise to supramolecular structures very similar to those found in natural elastic fibers (4, 5, 11). This self-aggregation property of tropoelastin is thought to contribute to elastic fiber assembly in vivo. However, self-aggregation alone is insufficient to explain the efficiency of the assembly process and the variable form of elastic fibers in different tissues.

The formation of elastic fibers has been proposed to require the deposition of tropoelastin on a preexisting scaffold, cross-linking of tropoelastin monomers by lysyl oxidase (LOX) family enzymes, and organization of the resulting insoluble elastin matrix into mature fibers (37). Fibrillin-rich microfibrils are thought to provide the scaffold for the deposition of elastin. Unexpectedly, normal elastic fiber assembly was found to occur in *fibrillin-1* or *fibrillin-2* mutant mice (2, 9, 42, 43). Therefore, the molecular mechanism of elastic fiber assembly remains elusive.

A significant insight into elastogenesis comes from two recent studies of *fibulin-5*$^{-/-}$ mice. These mice exhibit disrupted and disorganized elastic fibers throughout the body, indicating that fibulin-5 (also known as DANCE or EVEC) plays an important role in elastic fiber formation (40, 56). *fibulin-5*$^{-/-}$ mice grow to adulthood without lethality but have loose skin, vascular abnormalities, and emphysematous lungs. Fibulin-5 has an RGD motif and interacts with cell surface integrins and elastin. Thus, it has been proposed to promote elastic fiber formation by linking elastic fibers to cells (40, 56).

Fibulin-5 belongs to the fibulin family of six known ECM proteins that share tandem arrays of calcium-binding epidermal growth factor domains and a characteristic carboxyl-terminal fibulin domain (1, 10, 15, 52). Although little is known about the functions of fibulins, mutations of individual members have been associated with several diseases. A single mutation of an arginine to trypotophan in fibulin-3 (also known as

* Corresponding author. Mailing address: Department of Ophthalmology and Vision Science, University of Arizona, 655 N. Alvernon Way, Suite 108, Tucson, AZ 85711. Phone: (520) 626-0447. Fax: (520) 626-0457. E-mail: Lmarmorstein@eyes.arizona.edu.

† P.J.M. and Q.C. contributed equally to this work.

EFEMP1, S1-5, or FBNL) causes an inherited macular degenerative disease termed malattia leventinese or Doyne honeycomb retinal dystrophy (51). Missense variations in other fibulins have been detected in patients with age-related macular degeneration (47, 50), the most common cause of incurable blindness (6). Mutations in fibulin-5 have also been found in some cutis laxa patients (29, 32). So far, fibulin-5 is the only fibulin reported to be necessary for elastogenesis, whereas fibulin-1-null mice are reported to die perinatally as a result of hemorrhages, due to defects associated with capillary endothelial cells (25). Knockout mice for other fibulins have not been reported. Among the fibulins, fibulin-3, fibulin-4 (also known as EFEMP2, MBP1, H411, or UPH1), and fibulin-5 share highest homology with each other. These three fibulins are the smallest members of the family, share >50% amino acid identity, and are nearly identical in their structural organization (1, 10, 15, 52). Despite this homology, fibulin-5 deficiency is not compensated for by fibulin-3 or -4, suggesting that fibulin-3, -4, and -5 are not functionally redundant.

The function of fibulin-4 is poorly understood. Several studies have consistently found that fibulin-4 promotes cell growth, exhibits oncogenic properties, and is upregulated in tumor tissues (14, 16, 19). *fibulin-4* mRNA has been shown to be widely expressed in various tissues throughout the body (14, 16, 18). High protein levels are present in blood vessel walls (18). During development, *fibulin-4* mRNA is expressed in mouse embryos as early as embryonic day 7 (E7) (14). In this study, we investigated the biological role of fibulin-4 through targeted gene inactivation in mice. Remarkably, mice lacking fibulin-4 do not form elastic fibers, with resulting severe vascular and lung defects; they die perinatally. These results demonstrate that fibulin-4 plays an irreplaceable role in elastic fiber formation.

MATERIALS AND METHODS

***fibulin-4*$^{-/-}$ mouse generation, Southern blot analysis, and RT-PCR.** The targeting vector was constructed using 2.5-kb (5′) and 3-kb (3′) mouse *fibulin-4* genomic DNA fragments as homology arms. The two arms flanked a promoterless *lacZ* and a neomycin-resistant gene cassette (*lacZ-neo*). Homologous recombination in mouse embryonic stem cells resulted in the insertion of the *lacZ-neo* cassette into exon 4 of the mouse *fibulin-4* locus. Germ line-transmitting chimeric mice generated from the targeted embryonic stem cells were bred with C57BL/6 mice to produce F_1 *fibulin-4*$^{+/-}$ mice (Deltagen). Intercrossing of heterozygous F_1 mice generated F_2 *fibulin-4*$^{-/-}$ mice. Southern blot analysis was performed for identification of homologous recombinants. Genomic DNA was extracted using a DNA purification kit (Gentra) from mouse tail biopsy samples, digested with KpnI, separated on a 0.5% SeaKem Gold agarose (Cambrex) gel, and transferred to a Hybond-N$^+$ nylon membrane (Amersham) by capillary blotting. The membrane was hybridized with a 5′ or 3′ external probe that is outside of the homologous arm regions. The probes were labeled with ^{32}P through random priming using the Megaprime DNA Labeling system (Amersham). The labeled probes were purified using ProbeQuant G-50 Micro Columns (Amersham). Hybridization was performed using the MiracleHyb hybridization solution (Stratagene) according to the manufacturer's instructions. Reverse transcription-PCR (RT-PCR) was performed as described previously (33) to confirm the absence of *fibulin-4* expression in homozygous mice. Total RNA was isolated from wild-type, *fibulin-4*$^{+/-}$, and *fibulin-4*$^{-/-}$ mice at postnatal day 1 (P1). Either a 5′ or 3′ primer set corresponding to mouse *fibulin-4* cDNA sequence was used in the PCRs. The 5′ primer set (5′-GGCCAGATCTATGCTCCCTTT TGCCTCCTG-3′ and 5′-ACATCCACACAGCTCTCCTG-3′) generates a 381-bp fragment, and the 3′ primer set (5′-TGTCGAGAGCAGCCTTCA TC-3′ and 5′-GGCCGTCGACTCAGAAGGTATAGGCTCCCAC-3′) generates a 357-bp fragment. *fibulin-3* primers were used in the positive control.

Morphological and histological analyses. Timed pregnant mice were sacrificed by CO_2 asphyxiation for collection of embryos at E9.5 to E18.5. P1 pups were sacrificed by cervical dislocation. Sacrificed embryos or P1 mice were immobilized on agarose plates on their back. The ventral side of the embryos was gently dissected away to expose the aorta and other large arteries. Blood vessels were photographed with a dissecting microscope equipped with a charge-coupled device camera.

For histology, whole embryos and tissues dissected from newborn pups were fixed in Bouin's fixative or 4% paraformaldehyde in 0.1 M phosphate buffer (pH 7.2), dehydrated, and embedded in paraffin. Ten-micrometer sections were stained with hematoxylin and eosin or for elastin using elastin van Gieson stain (Sigma).

Transmission electron microscopy. Dissected tissues were fixed overnight in 3% glutaraldehyde in 0.144 M cacodylate buffer, pH 7.2. One-micrometer sections of plastic-embedded samples were cut and stained with methylene blue to examine the integrity of the tissue. Thin sections were cut on a Reichert Ultracut microtome, counterstained with uranyl acetate, and examined and photographed with a Philips CM-12S electron microscope.

Tissue desmosine assay. Tissue samples from P1 mice were collected from the thoracic aorta and lung. The tissues were hydrolyzed in 6 N HCl at 100°C for 24 h, evaporated to dryness, and redissolved in water. Desmosine was quantified by radioimmunoassay as previously described (49), and hydroxyproline was determined by amino acid analysis.

Northern blot analysis. Eight micrograms of total RNA isolated from various tissues of wild-type, *fibulin-4*$^{+/-}$, and *fibulin-4*$^{-/-}$ mice at P1 was separated on a 1% formaldehyde-agarose gel and transferred to a Hybond-XL nylon membrane (Amersham). Prehybridization was performed by incubating the membrane for 4 h at 65°C in the hybridization buffer without the probe. The membrane was hybridized with a ^{32}P-labeled probe using the Megaprime DNA Labeling system (Amersham). The *fibulin-4* probe is a 357-bp mouse *fibulin-4* cDNA fragment amplified by RT-PCR, the tropoelastin probe is a 3.6-kb mouse tropoelastin cDNA fragment containing the entire coding sequence released by SalI/NotI digestion from vector pCMV-SPORT6-mELN (Open Biosystems), and the LOX probe is a 4-kb mouse *Lox* cDNA fragment released by SalI-NotI digestion from vector pCMV-SPORT6-mLOX (Open Biosystems). After the *fibulin-4* probe was used, the same membranes were stripped by being boiled for 30 min in 0.1% sodium dodecyl sulfate (SDS), washed, and hybridized with other probes. A mouse glyceraldehyde-3-phosphate dehydrogenase (GAPDH) probe was used as a control. A 1.2-kb GAPDH fragment was generated by RT-PCR using the primers 5′-CCGCATCTTCTTGTGCAGTGCCA-3′ and 5′-CGAACTTTATTG ATGGTATTCAAGAGA.

Production of MAbs against human fibulin-4. cDNA encoding human fibulin-4 (OriGene Technologies) without signal peptide was cloned into vector pGEX-4T-2 (Pharmacia) to generate fibulin-4 fused with glutathione *S*-transferase (GST). GST–fibulin-4 or GST was purified as described previously (36). Four mice were immunized with GST–fibulin-4. Sera (polyclonal antibodies) from all the mice were characterized with both GST fusion proteins and lysates of transfected 293T cells expressing recombinant fibulin-4. Hybridomas were derived from one of these mice. Several different clones producing monoclonal antibodies (MAbs) against fibulin-4 were identified by enzyme-linked immunosorbent assay. Clones 7B9 (immunoglobulin G2a [IgG2a]) and 11E2 (IgG2b) are of high specificity and titer.

Transfection, immunoprecipitation, and immunoblotting. 293T cells were transfected with a control plasmid, pCMV6-XL4-fb4 (human *fibulin-4* cDNA), pCMV6-XL6-heln (human *tropoelastin* cDNA obtained from Origene), or both pCMV6-XL4-fb4 and pCMV6-XL6-heln with Lipofectamine (Invitrogen). At 48 h after transfection, cells were lysed. Immunoprecipitation and immunoblotting using antibodies against fibulin-4 and human elastin (Elastin Products Company) were performed as previously described (34) with modifications. To avoid the interference of the IgG heavy chain in interpreting results of immunoblotting following immunoprecipitation by the same or similar antibodies, immunoprecipitation was performed with antibodies covalently coupled to protein A-Sepharose. Anti-fibulin-4 MAb 7B9 or a rabbit anti-human tropoelastin polyclonal antibody (Elastin Products Company) was cross-linked to protein A-Sepharose CL-4B (Pharmacia) using dimethylpimelimidate (Sigma) as previously described (35). For each immunoprecipitation, cell lysate containing 200 μg of total protein was diluted to 1 ml with lysis buffer containing 50 mM Tris (pH 8.0), 150 mM NaCl, 10% glycerol, 0.5% NP-40, 0.5% Triton X-100, 1 mM phenylmethylsulfonyl fluoride, and a 1:100 dilution of protease inhibitor mixture III (Calbiochem). A total of 25 μl of antibody-protein A beads was incubated with the cell lysate for 4 h at 4°C. The immunoprecipitates were washed and resuspended in 30 μl of SDS-polyacrylamide gel electrophoresis (SDS-PAGE) sample buffer; 10 μl of the suspension was loaded to each well, resolved by SDS-PAGE on a 10% gel, and transferred onto a polyvinylidene difluoride membrane (Millipore). Anti-fibulin-4 MAb 11E2 or the anti-human tropoelastin antibody was used in immu-

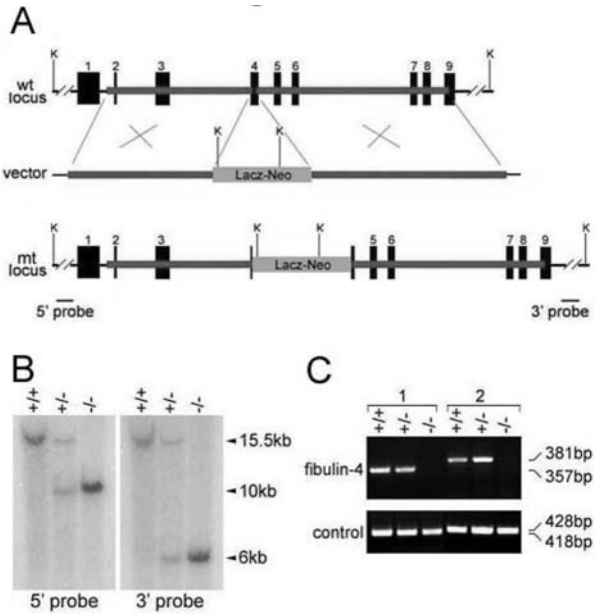

FIG. 1. Targeted disruption of the mouse *fibulin-4* gene. (A) Targeting strategy. Thick lines represent the homology arms used for constructing the targeting vector. Numbered solid boxes depict *fibulin-4* exons. The external 5′ and 3′ probes (B) are indicated as two bars beneath the mutant (mt) locus. wt, wild-type; K, KpnI. (B) Southern blot analysis of tail genomic DNA from wild-type (+/+), heterozygous (+/−), and homozygous (−/−) mice. The 15.5-kb wild-type band was detected by both 5′ and 3′ probes, the 10-kb mutant band was detected by the 5′ probe, and the 6-kb mutant band was detected by the 3′ probe. (C) RT-PCR analysis of mouse RNA. No PCR product was detected for homozygous mice with either a 3′ (1) or 5′ (2) primer set, indicating the absence of *fibulin-4* mRNA in these mice. In the positive control, PCR products were detected for all mice when a 3′ or 5′ primer set was used for fibulin-3.

noblotting. Alkaline phosphatase-conjugated anti-mouse IgG2b or anti-rabbit IgG (Jackson ImmunoResearch Laboratories) was used as a secondary antibody.

Production of recombinant fibulin-4 and solid-phase binding assay. Plasmid pEF6/V5 (Invitrogen) was modified to place a preprotrypsin signal sequence, a FLAG tag, and a His_6 tag to the N terminus of its inserted protein. Mouse *fibulin-4* cDNA without the signal sequence was subcloned to the modified vector. 293T cells were transfected with the resulting vector with Lipofectamine Plus (Invitrogen), according to the manufacturer's protocol. Stably transfected cells were selected with Blasticidin (Invitrogen). Recombinant fibulin-4 was purified from the serum-free conditioned medium of stable lines with TALON His-Tag Purification resins (Clontech) according to the manufacturer's instructions. The purity of the protein was confirmed by Coomassie blue staining of a SDS-PAGE gel, and the protein concentration was determined with Coomassie Plus reagent (Pierce). Various concentrations of purified fibulin-4 in Tris-buffered saline containing 2% skim milk with 2 mM $CaCl_2$ or 5 mM EDTA were used as ligands for a solid-phase binding assay. Recombinant bovine tropoelastin was prepared as previously described (26). Solid-phase binding assays using purified tropoelastin were performed as previously described (54) with the modification of 2 mM $CaCl_2$ or 10 mM EDTA added in the buffer. Anti-FLAG M2 antibody (Sigma) (1:2,000) was used as a primary antibody; horseradish peroxidase-conjugated anti-mouse IgG antibody (Santa Cruz) (1:3,000) was used as a secondary antibody. A color reaction assay was performed with the R&D Substrate Reagent Pack, followed by optic density measurement at 450 nm.

Cell culture and immunostaining. Normal human skin fibroblasts were cultured in Dulbecco's modified Eagle's medium with 10% fetal bovine serum at a density of 8×10^4 cells per 1 well of 24-well plate (day 0). On day 3, the medium was changed to Dulbecco's modified Eagle's medium-F12 with 10% fetal bovine serum and recombinant mouse fibulin-4 at a concentration of 5 μg/ml. On day 12, cells were fixed with 100% methanol and stained with rabbit antielastin antibody PR533 (1/100; Elastin Products Company) and mouse anti-FLAG M2 antibody (1/100; Sigma). Alexa Fluor 546-conjugated anti-rabbit IgG (1/100; Invitrogen) and Alexa Fluor 488-conjugated anti-mouse IgG (1/100; Invitrogen) were used as secondary antibodies. Stained cells were mounted with Vectashield with 4,6-diamino-2-phenylindole (DAPI) (Vector) and examined with a confocal microscope (Carl Zeiss).

RESULTS

Targeted inactivation of the *fibulin-4* gene results in perinatal lethality. The mouse *fibulin-4* gene was inactivated by insertion of a promoterless *lacZ* and a neomycin-resistant gene cassette into exon 4 (Fig. 1A). Homologous recombinants were identified by Southern blot analysis (Fig. 1B). The absence of *fibulin-4* mRNA was confirmed by RT-PCR (Fig. 1C) and Northern blot analysis (see Fig. 7). We found no adult homozygous offspring of *fibulin-4*$^{+/-}$ crossings, raising the possibility that ablation of fibulin-4 causes early lethality. Genotype analysis of offspring at several developmental stages indicated that the number of wild-type, heterozygous, and homozygous animals were distributed in a normal Mendelian pattern at embryonic stages E11.5 and E18.5 (Table 1). However, most *fibulin-4*$^{-/-}$ mice died during birth, only 10% survived to P1, and all the homozygous mice died by P2 (Table 1). The frequency of heterozygous animals was about twice that of the wild type and thus was not affected by the disruption of one *fibulin-4* allele. These results demonstrate that lack of fibulin-4 causes perinatal lethality in mice.

Severe vascular and lung defects in *fibulin-4*$^{-/-}$ mice. The gross appearances of wild-type, *fibulin-4*$^{+/-}$, and *fibulin-4*$^{-/-}$ mice at P1 were similar. However, on dissection, *fibulin-4*$^{-/-}$ mice exhibited severe vascular and lung defects. The arteries were tortuous, with irregularities including narrowing, dilatation, aneurysms, rupture, and resulting hemorrhages. The abnormalities were most severe in the aorta (Fig. 2B) and large arteries but occurred in other arteries as well. In addition, all live-born *fibulin-4*$^{-/-}$ mice were found to have expanded lungs. Histological examinations showed markedly enlarged distal airspaces, similar to those of emphysematous lungs (Fig. 2D). No obvious difference was observed in other organs. Despite the severe phenotype exhibited by homozygous animals, heterozygous (*fibulin-4*$^{+/-}$) mice are fertile, have a normal life span, and appear to be indistinguishable from the wild-type littermates.

The earliest abnormality appears in *fibulin-4*$^{-/-}$ embryos at E12.5. To determine the onset time of defects in *fibulin-4*$^{-/-}$ mice, we studied different developmental stages of the mice. The earliest abnormality noted was a uniformly narrowing of the descending aorta in *fibulin-4*$^{-/-}$ embryos at E12.5 (Fig. 3B). The outer diameter of the aorta in *fibulin-4*$^{-/-}$ mice was only

TABLE 1. Genotype frequency of offspring from *fibulin-4*$^{+/-}$ mouse breedings

Stage	No. of animals (%) of genotype:			Total no.
	+/+	+/−	−/−	
E11.5	16 (31)	23 (45)	12 (24)	51
E18.5	18 (21)	45 (52)	23 (27)	86
P1	33 (32)	61 (59)	10 (10)	104
P2	46 (32)	97 (67)	1 (<1)	144
P3	53 (31)	118 (69)	0	171

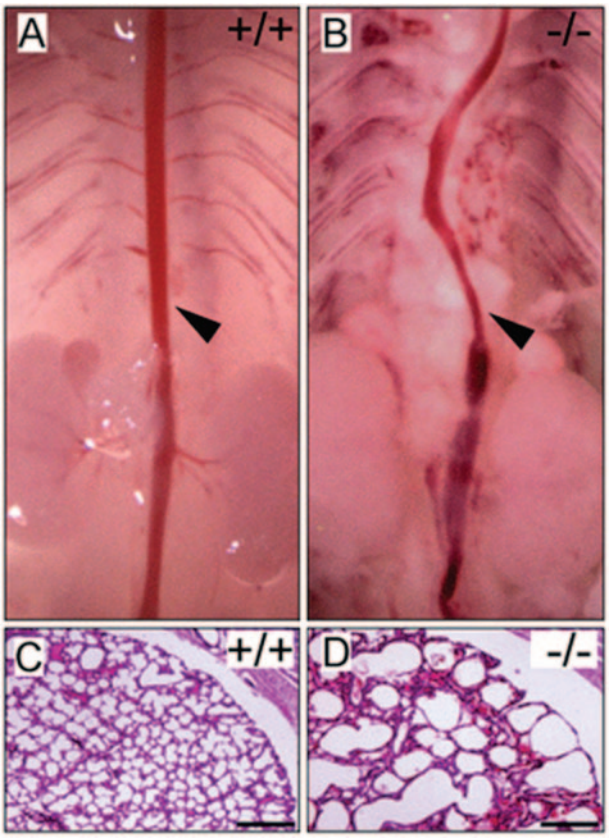

FIG. 2. Aorta and lung defects in *fibulin-4*$^{-/-}$ mice. (A and B) Aorta (arrowheads) of *fibulin-4*$^{+/+}$ and *fibulin-4*$^{-/-}$ mice at P1. (C and D) Hematoxylin and eosin staining of lung sections from mice at P1. The airspaces are significantly enlarged in *fibulin-4*$^{-/-}$ mice. Scale bars, 400 μm.

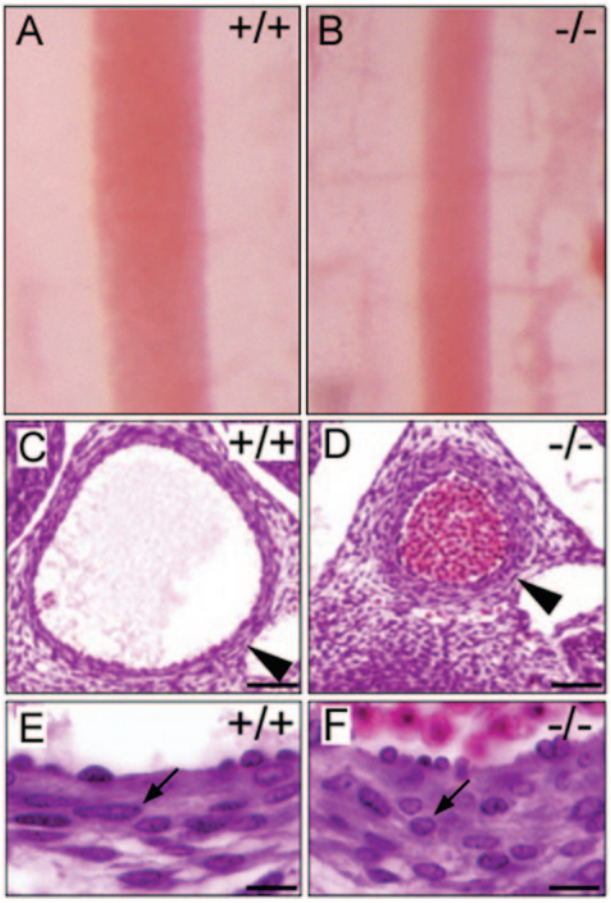

FIG. 3. The earliest abnormality in *fibulin-4*$^{-/-}$ mice at E12.5. (A and B) Aortas of *fibulin-4*$^{+/+}$ and *fibulin-4*$^{-/-}$ embryos at E12.5. (C to F) Hematoxylin and eosin staining of cross sections of descending aorta from E12.5 embryos. Note the smaller diameter and thicker wall of the *fibulin-4*$^{-/-}$ aorta (D). In contrast to the elongated, spindle-shaped cells (E, arrow) in wild-type mice, aortic wall cells were round in the *fibulin-4*$^{-/-}$ mice (F, arrow). Scale bars, 50 μm (C and D) and 20 μm (E and F).

one-half to two-thirds that of wild-type littermates. Histological analyses of cross sections showed that the aortic walls of *fibulin-4*$^{-/-}$ mice were nearly twice as thick as those of wild-type mice (Fig. 3D). However, the thickening of the *fibulin-4*$^{-/-}$ aortic wall did not appear to be the result of subendothelial overproliferation of cells, as the number of cells was similar in both *fibulin-4*$^{-/-}$ and wild-type aortic wall cross sections. There were 193 ± 3 cells for the wild type (data represent means and standard deviations for results with four mice) and 188 ± 7 cells for the homozygote (four mice) in a cross section of the aortic wall at a similar level of the thoracic aorta as shown in Fig. 3C and D. In contrast to the elongated and spindle-shaped cells in wild-type mice (Fig. 3E), the *fibulin-4*$^{-/-}$ aortic smooth muscle cells were round and appeared to be less stretched (Fig. 3F). The narrowing and the cell shape difference of the *fibulin-4*$^{-/-}$ aorta became less obvious at E13.5 and at older embryonic ages, likely due to passive expansion of the aorta caused by the dramatic increase in systemic blood pressure during these stages (22). Aortic tortuosity and irregularity were noticeable at E15.5 and became more pronounced with age in homozygous animals. These aorta abnormalities were not observed in *fibulin-4*$^{+/-}$ embryos.

***fibulin-4*$^{-/-}$ mice do not form elastic fibers.** The vascular and lung abnormalities of *fibulin-4*$^{-/-}$ mice were suggestive of elastic fiber defects. The appearance of abnormalities, coincident with the onset of elastogenesis in mice, suggests that genesis of elastic fibers may be impaired in *fibulin-4*$^{-/-}$ mice. Thus, we stained tissue sections from E12.5 to P1 with elastin van Gieson staining, which specifically stains elastic fibers. In the wild type, the innermost elastic lamina of the aorta was identifiable at E13.5 under a light microscope (Fig. 4A). By E14.5, four elastic laminae could be distinguished (Fig. 4C). All five elastic laminae were present at E16.5 or older ages (Fig. 4E and G). In contrast, no continuous elastic lamina was observed in the *fibulin-4*$^{-/-}$ aorta at any stage (Fig. 4B, D, F, and H). Instead, irregular elastin aggregates were visible at E14.5 (Fig. 4D), and more and larger aggregates accumulated with age (Fig. 4F and H). In the lung and skin, elastic fibers were not distinguishable by light microscopy at any embryonic stages. At P1, fine elastic fibers could be observed in lung and the hypodermal connective tissue of the skin of wild-type mice (Fig. 5A and C) but not in *fibulin-4*$^{-/-}$ mice (Fig. 5B and D). Despite this, the skin of *fibulin-4*$^{-/-}$ mice did not show obvious

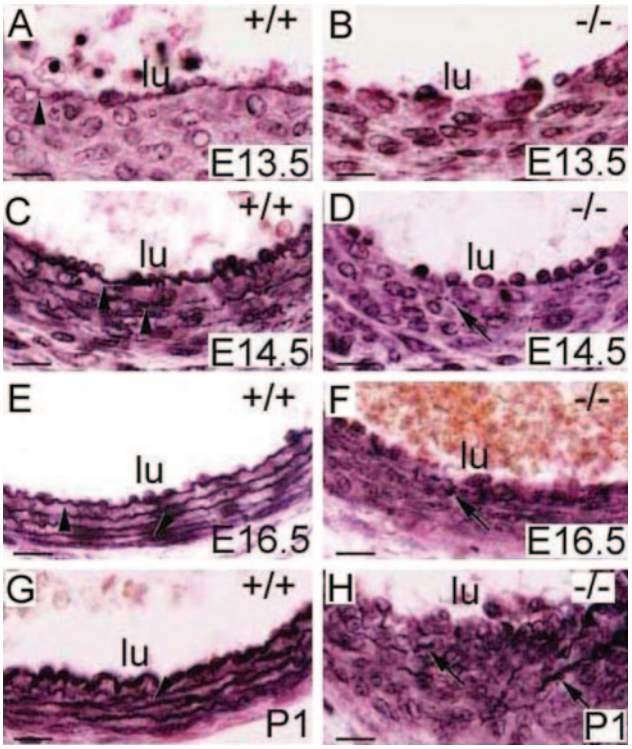

FIG. 4. Lack of elastic lamina in the *fibulin-4*$^{-/-}$ aorta. Elastin van Gieson staining of cross sections of descending aortae at different developmental stages is shown. The innermost elastic lamina (arrowheads) was identifiable in the wild-type aorta at E13.5 (A) and became more numerous and thicker at subsequent developing stages (C, E, and G). Only irregular elastin aggregates (arrows) were observed in the *fibulin-4*$^{-/-}$ aorta (B, D, F, and H). lu, lumen. Scale bars, 20 μm.

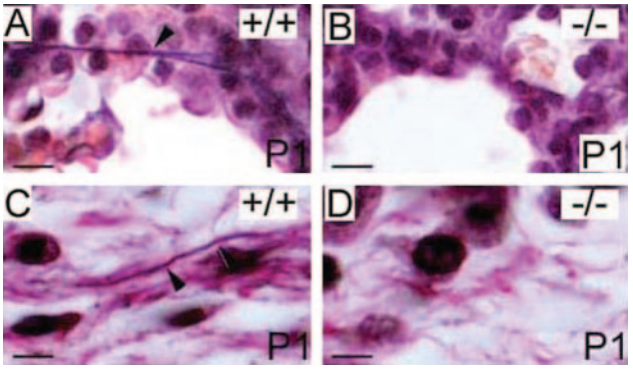

FIG. 5. Lack of elastic fibers in the skin and lung of *fibulin-4*$^{-/-}$ mice. (A and B) Elastin van Gieson staining of lung sections from P1 mice. Fine branched elastic fibers (arrowhead) were present in the wild-type (A) but not *fibulin-4*$^{-/-}$ (B) lung. (C and D) Elastin staining of skin sections from P1 mice. Elastic fibers were observed in the hypodermal connective tissue area of the wild-type skin (C, arrowhead) but not in the *fibulin-4*$^{-/-}$ skin (D). Scale bars, 10 μm (A and B) and 5 μm (C and D).

gross differences at this young age. Elastic fibers of *fibulin-4*$^{+/-}$ mice were similar to those of wild-type littermates. These results indicate that fibulin-4 is required for general elastogenesis.

Elastin aggregates containing electron dense rod-like filaments in *fibulin-4*$^{-/-}$ mice. To further understand the elastic fiber defects in *fibulin-4*$^{-/-}$ mice, we examined the aortae of E14.5 and P1 mice by electron microscopy (Fig. 6). Consistent with the finding by light microscopy, no intact elastic lamina was observed in the *fibulin-4*$^{-/-}$ aorta at either E14.5 or P1. Continuous elastic lamina was present in the wild-type aorta (Fig. 6A and C), but only irregular elastin aggregates were found in the *fibulin-4*$^{-/-}$ aorta at both stages (Fig. 6B and D, arrows). Noticeably, the content of the elastin aggregates appeared to be different from that of normal elastic fibers. Instead of an amorphous content, these elastin aggregates contained distinguishable electron-dense substances. Under higher magnification, dark rod-like filaments with similar sizes were seen to be evenly distributed in the elastin aggregates (Fig. 6F). These findings demonstrate that elastin does not properly assemble without fibulin-4.

Desmosine content is severely reduced in *fibulin-4*$^{-/-}$ mice. To determine whether mature elastin content is affected in *fibulin-4*$^{-/-}$ mice, we assessed the level of desmosine, an elastin cross-link-specific amino acid, in the aorta and lungs of wild-type, heterozygous, and homozygous mutant mice. As shown in Table 2, elastin cross-linking was nearly absent in *fibulin-4*$^{-/-}$ mice. There was a 94% decrease in the amount of desmosine in the aorta and 88% decrease in lungs of *fibulin-4*$^{-/-}$ mice compared with wild-type mice. Interestingly, there was a near 20% increase in the amount of desmosine in heterozygous mutants compared with wild-type mice (Table 2), although this difference was not statistically significant ($P > 0.05$ in a t test). We did not find any difference in the level of hydroxyproline, an indicator of collagen content, between wild-type and *fibulin-4*$^{-/-}$ mice (data not shown), indicating that the amount of collagen did not differ in *fibulin-4*$^{-/-}$ mice.

Tropoelastin and LOX expression is not affected in *fibulin-4*$^{-/-}$ mice. Elastin cross-linking is catalyzed by LOX family enzymes. Among the five known members, LOX has been shown to be necessary for elastic fiber development (20, 31). To determine whether lack of fibulin-4 causes elastinopathy by affecting tropoelastin or *Lox* expression, we examined the mRNA levels of *fibulin-4*, tropoelastin, and *Lox* in wild-type, heterozygous, and homozygous littermates at P1. As shown in Fig. 7, while heterozygotes showed reduced *fibulin-4* mRNA levels compared to those in wild-type mice and homozygotes had no detectable *fibulin-4* mRNA, all of them had similar levels of tropoelastin or *Lox* expression. Elastin has been shown to have an antiproliferative effect on vascular smooth muscle cells, and mice lacking elastin (*ELN*$^{-/-}$) die of vascular occlusion resulting from subendothelial cell proliferation (27). The unaffected tropoelastin expression is consistent with the lack of cell overproliferation and the accumulation of irregular elastin aggregates in *fibulin-4*$^{-/-}$ mice.

Fibulin-4 interacts with tropoelastin and assembles into elastic fibers. To investigate possible mechanisms by which fibulin-4 affects elastogenesis, we assessed the potential for interaction between fibulin-4 and elastin. Recombinant mouse fibulin-4 was expressed and purified from stably transfected 293T cell medium (Fig. 8A). A FLAG tag and a His_6 tag were added at the N terminus of fibulin-4 without its signal peptide to facilitate the purification and characterization of fibulin-4.

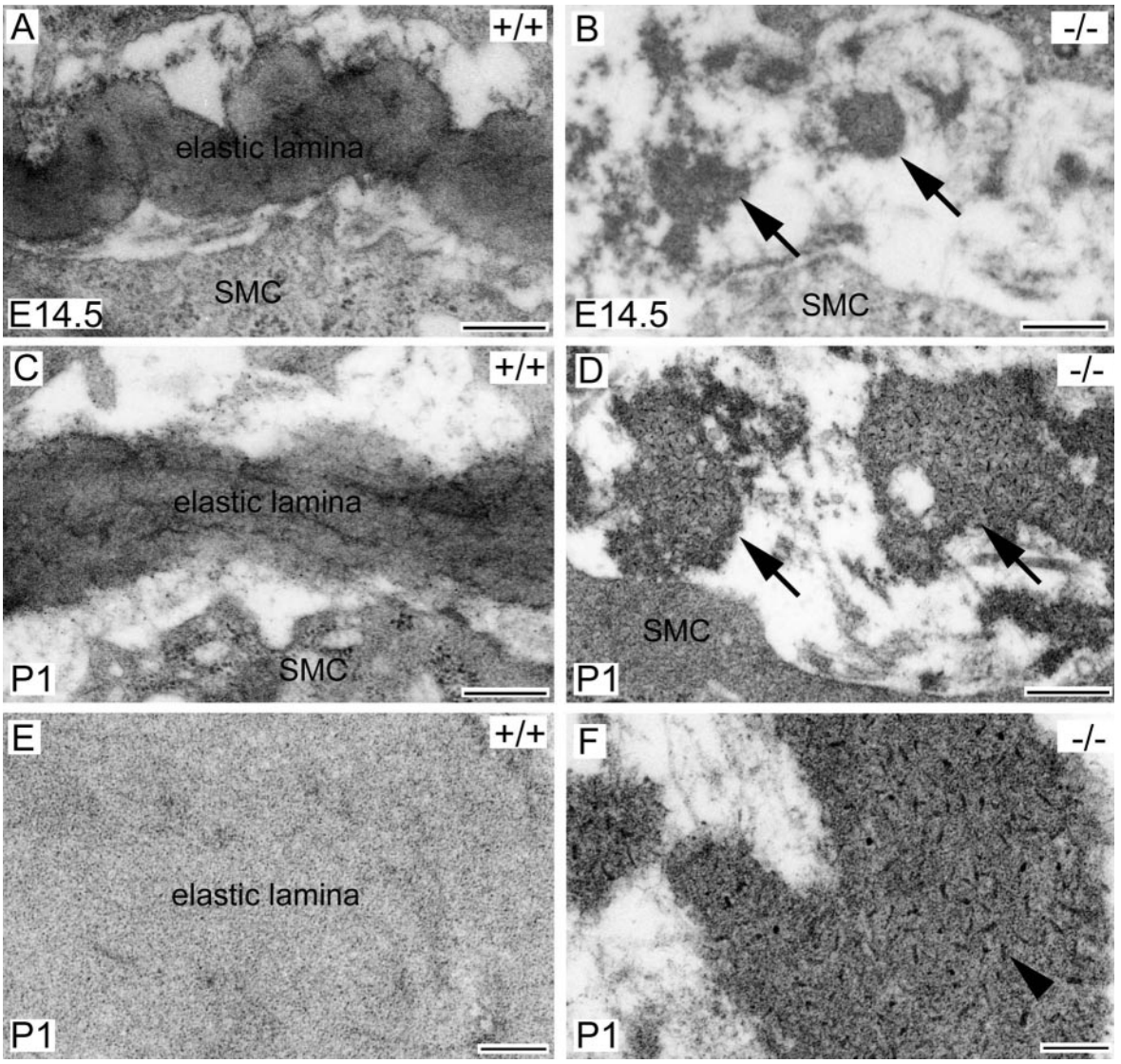

FIG. 6. Electron microscopy of elastic laminae in *fibulin-4*$^{-/-}$ mice. (A to D) Descending aorta cross sections from E14.5 (A and B) and P1 (C and D) mice. The wild-type aorta contained continuous elastic lamina (A and C). In contrast, irregular elastin aggregates (arrows) were randomly distributed in the *fibulin-4*$^{-/-}$ aorta (B and D). Under higher magnification (E and F), the wild-type elastic lamina appeared to be amorphous (E). But distinct, dark rod-like filaments (F, arrowhead) were evenly distributed in the *fibulin-4*$^{-/-}$ elastin aggregates. SMC, smooth muscle cell. Scale bars, 400 nm (A to D) and 100 nm (E and F).

The tagged protein was secreted from a preprotrypsin signal sequence. Although we found that untagged fibulin-4 was secreted efficiently from its native signal peptide, the C-terminal-tagged fibulin-4 was poorly secreted. It is possible that the C-terminal domain affects protein folding and is sensitive to modification. In a solid-phase binding assay, purified tropoelastin was used as an immobilized protein substrate, and fibulin-4 was used as a soluble ligand. As shown in Fig. 8B, fibulin-4 bound strongly to tropoelastin in the presence of Ca^{2+} and the binding was inhibited in the presence of EDTA, suggesting that calcium is required for the binding and the calcium-binding epidermal growth factor domains of fibulin-4 may be necessary for this binding. However, it has not been demonstrated experimentally that fibulin-4 binds calcium. No binding was observed between fibulin-4 and a control substrate (bovine serum albumin). These results indicate that fibulin-4 and tropoelastin can interact directly.

TABLE 2. Desmosine in picomoles per milligram of protein in aorta and lung at P1

Genotype (*n*)	Desmosine ± SD (% of wild type) in:	
	Aorta	Lung
+/+ (12)	419.05 ± 125.94 (100)	29.7 ± 14.87 (100)
+/− (21)	501.86 ± 133.85 (120)[a]	35.63 ± 9.08 (120)[b]
−/− (6)	25.35 ± 8.69 (6)[c]	3.15 ± 1.45 (12)[c]

[a] $P = 0.09$, compared to the wild type by *t* test.
[b] $P = 0.23$, compared to the wild type by *t* test.
[c] $P < 0.0001$, compared to the wild type by *t* test.

To assess whether fibulin-4 and tropoelastin interact in solution, we performed a coimmunoprecipitation assay. Human *fibulin-4* cDNA, human *tropoelastin* cDNA, or both were trans-

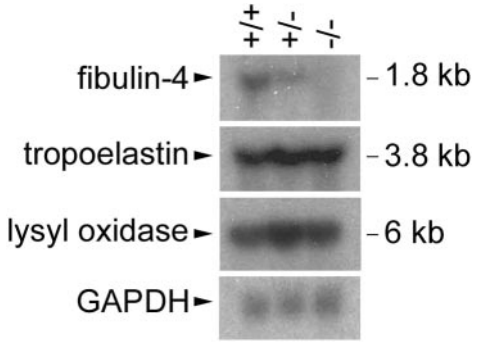

FIG. 7. Unaffected tropoelastin and lysyl oxidase expression in *fibulin-4*$^{-/-}$ mice. Northern blot analysis of equal amount of mouse lung total RNA shows a *fibulin-4* mRNA transcript of 1.8 kb detectable in wild-type (+/+) and heterozygous (+/−) but not homozygous (−/−) mice (top). The intensity of the signal is reduced in heterozygous mice. The same blot stripped and reblotted with a tropoelastin probe shows a 3.8-kb tropoelastin transcript with similar intensity in all the mice (second panel from the top). Probing with a *Lox* probe indicates a 6-kb *Lox* transcript with similar levels in all mice (third panel). A GAPDH probe was used as a control (bottom).

fected into 293T cells. Tropoelastin was expressed at a very low level. We could detect tropoelastin in the cell lysate, but it was difficult to detect it in the culture medium, presumably due to its self-coacervation and formation of insoluble elastin in the medium. Fibulin-4 was expressed at a relatively high level and could be readily detected in both lysate and medium. Thus, we chose to use transfected cell lysates for the coimmunoprecipitation assay. As shown in Fig. 8C, tropoelastin was immunoprecipitated from lysates transfected with either tropoelastin alone (lane 2) or both tropoelastin and fibulin-4 (lane 1) by the antitropoelastin antibody. It was also coimmunoprecipitated by an anti-fibulin-4 monoclonal antibody from the lysate cotransfected with tropoelastin and fibulin-4 (lane 3). The coimmunoprecipitation did not appear to be due to a nonspecific association of tropoelastin with the fibulin-4 antibody beads, as no tropoelastin signal was detected from the immunoprecipitate by the same antibody from the lysate transfected only with tropoelastin (lane 4). Reciprocally, fibulin-4 was coimmunoprecipitated by the anti-tropoelastin antibody from the lysate transfected with both tropoelastin and fibulin-4 (lane 7) but not from the lysate transfected with fibulin-4 alone (lane 8), while it was immunoprecipitated by the fibulin-4 antibody from both lysates (lanes 5 and 6). These results demonstrate that fibulin-4 binds specifically with tropoelastin.

To further determine whether exogenous fibulin-4 is colocalized to elastic fibers, we added FLAG-tagged recombinant fibulin-4 to cultured human fibroblasts. These cells are capable of developing a network of elastic fibers in vitro. Double labeling of antitropoelastin and anti-FLAG antibodies showed colocalization of fibulin-4 and elastin (Fig. 9). These data indicate that fibulin-4 assembles into elastic fibers.

DISCUSSION

Elastic fiber formation is thought to involve extrinsic proteins and an intrinsic capacity for elastin coacervation. How extrinsic proteins cooperate with each other and with elastin coacervation to form functional elastic fibers is unknown. Over 30 molecules have been reported to associate with elastic fibers in morphological studies and in vitro assays (23). But many

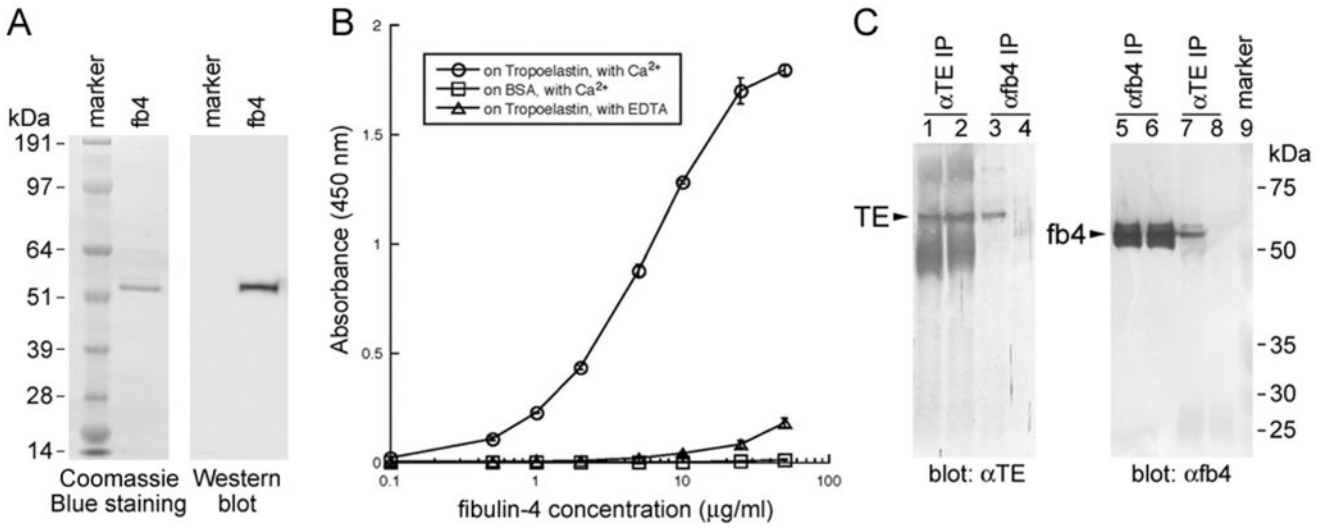

FIG. 8. Fibulin-4 interacts with tropoelastin. (A) Purified recombinant mouse fibulin-4. A total of 1 μg of purified fibulin-4 was used for the Coomassie blue-stained gel, and 10 ng of the protein was used for the Western blot. An anti-FLAG antibody was used for immunodetection. A single band with the correct mass for fibulin-4 was detected by both Coomassie blue staining and immunoblotting. (B) Solid-phase binding assay using recombinant fibulin-4 as a soluble ligand. Note that fibulin-4 binds to tropoelastin in the presence of Ca^{2+} but that the binding is inhibited in the presence of EDTA. Data were obtained as the results of triplicate experiments, and values shown are means ± standard deviations. (C) Coimmunoprecipitation of fibulin-4 with tropoelastin. Lanes 1 to 4, antitropoelastin blotting of immunoprecipitates from lysates of 293T cells transfected with both tropoelastin and fibulin-4 (lanes 1 and 3) or tropoelastin alone (lanes 2 and 4). Tropoelastin was detected in the immunoprecipitate by anti-fibulin-4 (7B9) (lane 3). Lanes 5 to 8, anti-fibulin-4 (11E2) blotting of immunoprecipitates from lysates of 293T cells transfected with both tropoelastin and fibulin-4 (lanes 5 and 7) or fibulin-4 alone (lanes 6 and 8). Fibulin-4 was detected in the immunoprecipitate by antitropoelastin (lane 7). IP, immunoprecipitation; TE, tropoelastin; fb4, fibulin-4.

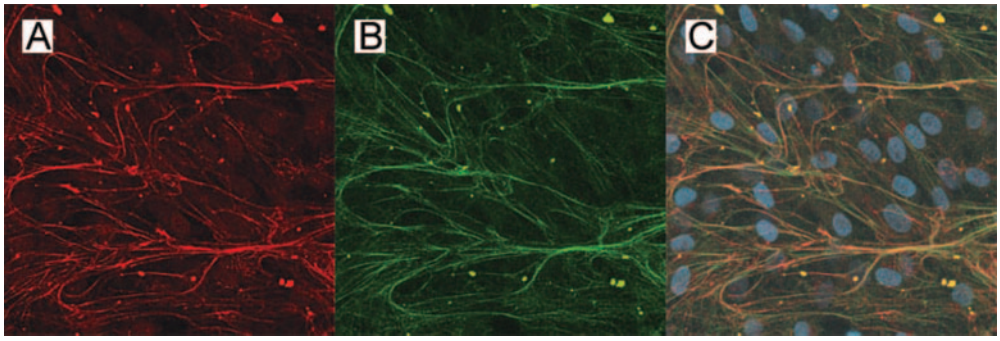

FIG. 9. Colocalization of fibulin-4 and elastin. (A to C) Normal human skin fibroblasts were cultured with FLAG-tagged recombinant fibulin-4 protein. (A) Cells stained with antitropoelastin antibody, showing a network structure. (B) Cells stained with anti-FLAG antibody, also showing a network structure. (C) Superimposed image of panels A and B, with DAPI nuclear staining showing fibulin-4 localization on elastic fibers.

have been found to have no effect or marginal effects on elastic fiber formation in vivo. In this study, we demonstrated that mice lacking fibulin-4 do not form elastic fibers. This is the first report that lack of a protein other than elastin itself completely abolishes the formation of elastic fibers in vivo, indicating that fibulin-4 plays an indispensable role in elastogenesis.

The initial abnormality present in *fibulin-4*$^{-/-}$ mice, arterial narrowing, is similar to that observed with *ELN*$^{-/-}$ mice (27). In *ELN*$^{-/-}$ mice, however, the change is caused by subendothelial cell overproliferation due to the lack of elastin, a process that eventually obliterates the vascular lumen (27). In *fibulin-4*$^{-/-}$ mice, tropoelastin mRNA levels are similar to those in wild-type mice, there is no sign of cell overproliferation and vascular occlusion, and irregular elastin aggregates accumulate with age, suggesting that fibulin-4 does not affect the synthesis of tropoelastin. The formation of functional elastic fibers requires the deposition of tropoelastin at the fiber assembly site, cross-linking of tropoelastin monomers by lysyl oxidase family enzymes, and the organization of resulting insoluble elastin matrix into mature fibers. Fibulin-4 likely affects one or more of these processes.

The irregular elastin aggregates observed in *fibulin-4*$^{-/-}$ mice are highly unusual in that they contain electron-dense rod-like filaments. These filaments are evenly distributed in the aggregates in *fibulin-4*$^{-/-}$ mice, as if, without fibulin-4, a molecule(s) associated with tropoelastin is incorporated together with each tropoelastin monomer into elastin aggregates. Alternatively, the rod-like filament may be a regular elastic fiber component whose presence is revealed by the absence of fibulin-4. The morphology of *fibulin-4*$^{-/-}$ elastin aggregates is similar to that of abnormal elastin aggregates permeated by proteoglycans in the presence of lysyl oxidase inhibitors (13). Also, ECM proteoglycans containing sulfated glycosaminoglycans visualized by a cationic copper phthalocyanin dye, cupromeronic blue, exhibit morphology very similar to the rod-like filaments observed in irregular elastin aggregates in *fibulin-4*$^{-/-}$ mice (48). These observations suggest that the filaments in *fibulin-4*$^{-/-}$ elastin aggregates may be proteoglycans. Glycosaminoglycans containing sulfate groups (chondroitin, dermatan, and heparan sulfate) and their associated proteoglycans have been shown to directly interact with tropoelastin and are normal components of elastic fibers (3, 7, 17, 55). Both chondroitin sulfate and heparan sulfate can mediate tropoelastin's coacervation (17, 24, 45, 53, 55). Decreased elastin deposition was observed when the matrix was depleted of sulfated molecules by chlorate treatment of the cells (8, 53). We also found that fibulin-4 interacts with tropoelastin directly and assembles into elastic fibers in culture. Thus, fibulin-4 may play a role in the initial deposition of tropoelastin, such as scaffolding and facilitating the formation of homogeneous elastin polymers by preventing the association of other molecules with tropoelastin or coordinating tropoelastin and other elastic fiber components during elastic fiber assembly. The identity of the rod-like filaments, the precise roles of proteoglycans in elastogenesis, and their relationships with fibulin-4 remain to be determined.

Elastin cross-linking is severely affected in *fibulin-4*$^{-/-}$ mice. Desmosine was reduced by over 85% in *fibulin-4*$^{-/-}$ mice, compared to levels in wild-type mice. Interestingly, there was a near-20% increase in desmosine in *fibulin-4*$^{+/-}$ mice compared to wild-type mice, although this difference was not statistically significant with the number of animals we analyzed. It is possible that there is more cross-linking in heterozygous mutants than in wild-type mice to compensate for fibulin-4 haploinsufficiency. Elastin cross-linking is catalyzed by lysyl oxidases, a family of enzymes that catalyzes the oxidative deamination of lysine residues in elastin and collagen (21). Five members have been described so far (12, 30). LOX has been shown to be necessary for elastic fiber and collagen fiber development (20, 31), and LOX-like 1 (LOXL1) is required in elastic fiber homeostasis (28). Similar to *fibulin-4*$^{-/-}$ mice, *Lox*$^{-/-}$ mice exhibit severe vascular defects and die perinatally (20, 31). The vascular defects include artery tortuosity, irregularity, and ruptured aneurysms with fragmented elastic lamina in the aortic walls. Desmosine content is decreased by 60%; hydroxyproline, which represents collagen content, is decreased by 30% in *Lox*$^{-/-}$ mice (20). The similarities in gross defects between *fibulin-4*$^{-/-}$ mice and *Lox*$^{-/-}$ mice and loss of desmosine content in *fibulin-4*$^{-/-}$ mice suggest that lack of fibulin-4 may affect the function of lysyl oxidase. However, *Lox* mRNA expression is similar in wild-type and *fibulin-4*$^{-/-}$ mice, hydroxyproline content is not altered in *fibulin-4*$^{-/-}$ mice, and no unusual elastic fiber content such as rod-like filaments found in *fibulin-4*$^{-/-}$ mice has been reported with *Lox*$^{-/-}$ mice. Loxl1-null mice survive to adulthood but do not deposit normal elastic fibers in the uterine tract postpartum; they develop

pelvic prolapse, enlarged airspaces of the lung, loose skin, and vascular abnormalities. Desmosine content in *Loxl1*$^{-/-}$ mice is reduced by 30 to 50%, depending on tissues (28). The difference in elastic fiber defects in *fibulin-4*$^{-/-}$, *Lox*$^{-/-}$, and *Loxl1*$^{-/-}$ mice suggests that fibulin-4 has different roles in elastic fiber assembly, even if it also affects the activities of lysyl oxidases.

Fibulin-4 shares high homology with fibulin-5, with a similar domain structure and >50% amino acid identity. Fibulin-5-null mice grow to adulthood but exhibit loose skin, lung airspace enlargement, and a stiff and tortuous aorta, due to disorganized and fragmented elastic fibers (40, 56). It has been proposed that fibulin-5 may be involved in elastogenesis by tethering elastic fibers onto cell surface integrins and by affecting cross-linking of elastin through direct binding with LOXL1 (28, 40, 56). *Loxl1*$^{-/-}$ mice exhibit similar but less-severe elastic fiber defects than *fibulin-5*$^{-/-}$ mice. Despite the high homology between fibulin-4 and -5, the *fibulin-4*$^{-/-}$ phenotype is not compensated for by fibulin-5. *fibulin-4*$^{-/-}$ mice exhibited almost complete loss of elastic fibers and perinatal lethality, suggesting a more essential role of fibulin-4 in elastogenesis than that of fibulin-5.

With age and some pathological conditions, elastic fibers exhibit interwoven filaments (41) that are similar to the morphology of elastin aggregates of *fibulin-4*$^{-/-}$ mice. Thus, alteration of the function or structure of fibulin-4 may be a major mechanism behind aging and elastic fiber-related diseases. *fibulin-4*$^{-/-}$ mice exhibit the most severe elastinopathy described to date. Understanding the role of fibulin-4 is a prerequisite for understanding the mechanism responsible for elastogenesis. In addition to the crucial role in elastogenesis, fibulin-4 may also have other important functions in cell proliferation and differentiation. Several studies have found that fibulin-4 stimulates cell growth and is upregulated in tumors (14, 16, 19). *fibulin-4*$^{-/-}$ mice will also be a valuable model in further studying these functions.

ACKNOWLEDGMENTS

We thank Peggy McCuskey for electron microscopy and Anna Yocom for technical assistance.

This work was supported by NIH/NEI grants EY13847 and EY13160, Research to Prevent Blindness, Philip Morris USA and Philip Morris International, Health and Labor Sciences research grants, Japan Society for the Promotion of Science, and Japan Science and Technology Agency.

REFERENCES

1. **Argraves, W. S., L. M. Greene, M. A. Cooley, and W. M. Gallagher.** 2003. Fibulins: physiological and disease perspectives. EMBO Rep. **4:**1127–1131.
2. **Arteaga-Solis, E., B. Gayraud, S. Y. Lee, L. Shum, L. Sakai, and F. Ramirez.** 2001. Regulation of limb patterning by extracellular microfibrils. J. Cell Biol. **154:**275–281.
3. **Baccarani-Contri, M., D. Vincenzi, F. Cicchetti, G. Mori, and I. Pasquali-Ronchetti.** 1990. Immunocytochemical localization of proteoglycans within normal elastin fibers. Eur. J. Cell Biol. **53:**305–312.
4. **Bressan, G. M., I. Castellani, M. G. Giro, D. Volpin, C. Fornieri, and I. Pasquali Ronchetti.** 1983. Banded fibers in tropoelastin coacervates at physiological temperatures. J. Ultrastruct. Res. **82:**335–340.
5. **Bressan, G. M., I. Pasquali-Ronchetti, C. Fornieri, F. Mattioli, I. Castellani, and D. Volpin.** 1986. Relevance of aggregation properties of tropoelastin to the assembly and structure of elastic fibers. J. Ultrastruct. Mol. Struct. Res. **94:**209–216.
6. **Bressler, N. M., S. B. Bressler, and S. L. Fine.** 1988. Age-related macular degeneration. Surv. Ophthalmol. **32:**375–413.
7. **Broekelmann, T. J., B. A. Kozel, H. Ishibashi, C. C. Werneck, F. W. Keeley, L. Zhang, and R. P. Mecham.** 2005. Tropoelastin interacts with cell-surface glycosaminoglycans via its COOH-terminal domain. J. Biol. Chem. **280:**40939–40947.
8. **Buczek-Thomas, J. A., C. L. Chu, C. B. Rich, P. J. Stone, J. A. Foster, and M. A. Nugent.** 2002. Heparan sulfate depletion within pulmonary fibroblasts: implications for elastogenesis and repair. J. Cell Physiol. **192:**294–303.
9. **Chaudhry, S. S., J. Gazzard, C. Baldock, J. Dixon, M. J. Rock, G. C. Skinner, K. P. Steel, C. M. Kielty, and M. J. Dixon.** 2001. Mutation of the gene encoding fibrillin-2 results in syndactyly in mice. Hum. Mol. Genet. **10:**835–843.
10. **Chu, M. L., and T. Tsuda.** 2004. Fibulins in development and heritable disease. Birth Defects Res. C Embryo Today **72:**25–36.
11. **Cox, B. A., B. C. Starcher, and D. W. Urry.** 1974. Communication: coacervation of tropoelastin results in fiber formation. J. Biol. Chem. **249:**997–998.
12. **Csiszar, K.** 2001. Lysyl oxidases: a novel multifunctional amine oxidase family. Prog. Nucleic Acid Res. Mol. Biol. **70:**1–32.
13. **Fornieri, C., M. Baccarani-Contri, D. Quaglino, Jr., and I. Pasquali-Ronchetti.** 1987. Lysyl oxidase activity and elastin/glycosaminoglycan interactions in growing chick and rat aortas. J. Cell Biol. **105:**1463–1469.
14. **Gallagher, W. M., M. Argentini, V. Sierra, L. Bracco, L. Debussche, and E. Conseiller.** 1999. MBP1: a novel mutant p53-specific protein partner with oncogenic properties. Oncogene **18:**3608–3616.
15. **Gallagher, W. M., C. A. Currid, and L. C. Whelan.** 2005. Fibulins and cancer: friend or foe? Trends Mol. Med. **11:**336–340.
16. **Gallagher, W. M., L. M. Greene, M. P. Ryan, V. Sierra, A. Berger, P. Laurent-Puig, and E. Conseiller.** 2001. Human fibulin-4: analysis of its biosynthetic processing and mRNA expression in normal and tumour tissues. FEBS Lett. **489:**59–66.
17. **Gheduzzi, D., D. Guerra, B. Bochicchio, A. Pepe, A. M. Tamburro, D. Quaglino, S. Mithieux, A. S. Weiss, and I. Pasquali Ronchetti.** 2005. Heparan sulphate interacts with tropoelastin, with some tropoelastin peptides and is present in human dermis elastic fibers. Matrix Biol. **24:**15–25.
18. **Giltay, R., R. Timpl, and G. Kostka.** 1999. Sequence, recombinant expression and tissue localization of two novel extracellular matrix proteins, fibulin-3 and fibulin-4. Matrix Biol. **18:**469–480.
19. **Heine, H., R. L. Delude, B. G. Monks, T. Espevik, and D. T. Golenbock.** 1999. Bacterial lipopolysaccharide induces expression of the stress response genes hop and H411. J. Biol. Chem. **274:**21049–21055.
20. **Hornstra, I. K., S. Birge, B. Starcher, A. J. Bailey, R. P. Mecham, and S. D. Shapiro.** 2003. Lysyl oxidase is required for vascular and diaphragmatic development in mice. J. Biol. Chem. **278:**14387–14393.
21. **Kagan, H. M., and P. C. Trackman.** 1991. Properties and function of lysyl oxidase. Am. J. Respir. Cell Mol. Biol. **5:**206–210.
22. **Kaufman, M. H., and J. B. L. Bard.** 1999. The Anatomical basis of mouse development. Academic Press, London, United Kingdom.
23. **Kielty, C. M., M. J. Sherratt, and C. A. Shuttleworth.** 2002. Elastic fibres. J. Cell Sci. **115:**2817–2828.
24. **Kielty, C. M., S. P. Whittaker, and C. A. Shuttleworth.** 1996. Fibrillin: evidence that chondroitin sulphate proteoglycans are components of microfibrils and associate with newly synthesised monomers. FEBS Lett. **386:**169–173.
25. **Kostka, G., R. Giltay, W. Bloch, K. Addicks, R. Timpl, R. Fassler, and M. L. Chu.** 2001. Perinatal lethality and endothelial cell abnormalities in several vessel compartments of fibulin-1-deficient mice. Mol. Cell. Biol. **21:**7025–7034.
26. **Kozel, B. A., H. Wachi, E. C. Davis, and R. P. Mecham.** 2003. Domains in tropoelastin that mediate elastin deposition in vitro and in vivo. J. Biol. Chem. **278:**18491–18498.
27. **Li, D. Y., B. Brooke, E. C. Davis, R. P. Mecham, L. K. Sorensen, B. B. Boak, E. Eichwald, and M. T. Keating.** 1998. Elastin is an essential determinant of arterial morphogenesis. Nature **393:**276–280.
28. **Liu, X., Y. Zhao, J. Gao, B. Pawlyk, B. Starcher, J. A. Spencer, H. Yanagisawa, J. Zuo, and T. Li.** 2004. Elastic fiber homeostasis requires lysyl oxidase-like 1 protein. Nat. Genet. **36:**178–182.
29. **Loeys, B., L. Van Maldergem, G. Mortier, P. Coucke, S. Gerniers, J. M. Naeyaert, and A. De Paepe.** 2002. Homozygosity for a missense mutation in fibulin-5 (FBLN5) results in a severe form of cutis laxa. Hum. Mol. Genet. **11:**2113–2118.
30. **Maki, J. M., and K. I. Kivirikko.** 2001. Cloning and characterization of a fourth human lysyl oxidase isoenzyme. Biochem. J. **355:**381–387.
31. **Maki, J. M., J. Rasanen, H. Tikkanen, R. Sormunen, K. Makikallio, K. I. Kivirikko, and R. Soininen.** 2002. Inactivation of the lysyl oxidase gene Lox leads to aortic aneurysms, cardiovascular dysfunction, and perinatal death in mice. Circulation **106:**2503–2509.
32. **Markova, D., Y. Zou, F. Ringpfeil, T. Sasaki, G. Kostka, R. Timpl, J. Uitto, and M. L. Chu.** 2003. Genetic heterogeneity of cutis laxa: a heterozygous tandem duplication within the fibulin-5 (FBLN5) gene. Am. J. Hum. Genet. **72:**998–1004.
33. **Marmorstein, A. D., L. Y. Marmorstein, M. Rayborn, X. Wang, J. G. Hollyfield, and K. Petrukhin.** 2000. Bestrophin, the product of the Best vitelliform macular dystrophy gene (*VMD2*), localizes to the basolateral plasma membrane of the retinal pigment epithelium. Proc. Natl. Acad. Sci. USA **97:**12758–12763.

34. **Marmorstein, L. Y., A. V. Kinev, G. K. Chan, D. A. Bochar, H. Beniya, J. A. Epstein, T. J. Yen, and R. Shiekhattar.** 2001. A human BRCA2 complex containing a structural DNA binding component influences cell cycle progression. Cell **104:**247–257.
35. **Marmorstein, L. Y., P. J. McLaughlin, J. B. Stanton, L. Yan, J. W. Crabb, and A. D. Marmorstein.** 2002. Bestrophin interacts physically and functionally with protein phosphatase 2A. J. Biol. Chem. **277:**30591–30597.
36. **Marmorstein, L. Y., F. L. Munier, Y. Arsenijevic, D. F. Schorderet, P. J. McLaughlin, D. Chung, E. Traboulsi, and A. D. Marmorstein.** 2002. Aberrant accumulation of EFEMP1 underlies drusen formation in malattia leventinese and age-related macular degeneration. Proc. Natl. Acad. Sci. USA **99:**13067–13072.
37. **Mecham, R. P., and E. Davis.** 1994. Elastic fiber structure and assembly, p. 281–314. *In* P. D. Yurchenco, D. E. Birk, and R. P. Mecham (ed.), Extracellular matrix assembly and structure. Academic Press, New York, N.Y.
38. **Midwood, K. S., and J. E. Schwarzbauer.** 2002. Elastic fibers: building bridges between cells and their matrix. Curr. Biol. **12:**R279–R281.
39. **Milewicz, D. M., Z. Urban, and C. Boyd.** 2000. Genetic disorders of the elastic fiber system. Matrix Biol. **19:**471–480.
40. **Nakamura, T., P. R. Lozano, Y. Ikeda, Y. Iwanaga, A. Hinek, S. Minamisawa, C. F. Cheng, K. Kobuke, N. Dalton, Y. Takada, K. Tashiro, J. Ross, Jr., T. Honjo, and K. R. Chien.** 2002. Fibulin-5/DANCE is essential for elastogenesis in vivo. Nature **415:**171–175.
41. **Pasquali-Ronchetti, I., and M. Baccarani-Contri.** 1997. Elastic fiber during development and aging. Microsc. Res. Tech. **38:**428–435.
42. **Pereira, L., K. Andrikopoulos, J. Tian, S. Y. Lee, D. R. Keene, R. Ono, D. P. Reinhardt, L. Y. Sakai, N. J. Biery, T. Bunton, H. C. Dietz, and F. Ramirez.** 1997. Targetting of the gene encoding fibrillin-1 recapitulates the vascular aspect of Marfan syndrome. Nat. Genet. **17:**218–222.
43. **Pereira, L., S. Y. Lee, B. Gayraud, K. Andrikopoulos, S. D. Shapiro, T. Bunton, N. J. Biery, H. C. Dietz, L. Y. Sakai, and F. Ramirez.** 1999. Pathogenetic sequence for aneurysm revealed in mice underexpressing fibrillin-1. Proc. Natl. Acad. Sci. USA **96:**3819–3823.
44. **Pierce, R. A., T. J. Mariani, and R. M. Senior.** 1995. Elastin in lung development and disease. Ciba Found. Symp. **192:**199–212.
45. **Reinboth, B., E. Hanssen, E. G. Cleary, and M. A. Gibson.** 2002. Molecular interactions of biglycan and decorin with elastic fiber components: biglycan forms a ternary complex with tropoelastin and microfibril-associated glycoprotein 1. J. Biol. Chem. **277:**3950–3957.
46. **Rosenbloom, J., W. R. Abrams, and R. Mecham.** 1993. Extracellular matrix 4: the elastic fiber. FASEB J. **7:**1208–1218.
47. **Schultz, D. W., M. L. Klein, A. J. Humpert, C. W. Luzier, V. Persun, M. Schain, A. Mahan, C. Runckel, M. Cassera, V. Vittal, T. M. Doyle, T. M. Martin, R. G. Weleber, P. J. Francis, and T. S. Acott.** 2003. Analysis of the ARMD1 locus: evidence that a mutation in HEMICENTIN-1 is associated with age-related macular degeneration in a large family. Hum. Mol. Genet **12:**3315–3323.
48. **Scott, J. E.** 1980. Collagen-proteoglycan interactions. Localization of proteoglycans in tendon by electron microscopy. Biochem. J. **187:**887–891.
49. **Starcher, B., and M. Conrad.** 1995. A role for neutrophil elastase in the progression of solar elastosis. Connect. Tissue Res. **31:**133–140.
50. **Stone, E. M., T. A. Braun, S. R. Russell, M. H. Kuehn, A. J. Lotery, P. A. Moore, C. G. Eastman, T. L. Casavant, and V. C. Sheffield.** 2004. Missense variations in the fibulin 5 gene and age-related macular degeneration. N. Engl. J. Med. **351:**346–353.
51. **Stone, E. M., A. J. Lotery, F. L. Munier, E. Heon, B. Piguet, R. H. Guymer, K. Vandenburgh, P. Cousin, D. Nishimura, R. E. Swiderski, G. Silvestri, D. A. Mackey, G. S. Hageman, A. C. Bird, V. C. Sheffield, and D. F. Schorderet.** 1999. A single EFEMP1 mutation associated with both malattia leventinese and Doyne honeycomb retinal dystrophy. Nat. Genet. **22:**199–202.
52. **Timpl, R., T. Sasaki, G. Kostka, and M. L. Chu.** 2003. Fibulins: a versatile family of extracellular matrix proteins. Nat Rev. Mol. Cell Biol. **4:**479–489.
53. **Trask, B. C., T. M. Trask, T. Broekelmann, and R. P. Mecham.** 2000. The microfibrillar proteins MAGP-1 and fibrillin-1 form a ternary complex with the chondroitin sulfate proteoglycan decorin. Mol. Biol. Cell **11:**1499–1507.
54. **Trask, T. M., B. C. Trask, T. M. Ritty, W. R. Abrams, J. Rosenbloom, and R. P. Mecham.** 2000. Interaction of tropoelastin with the amino-terminal domains of fibrillin-1 and fibrillin-2 suggests a role for the fibrillins in elastic fiber assembly. J. Biol. Chem. **275:**24400–24406.
55. **Wu, W. J., B. Vrhovski, and A. S. Weiss.** 1999. Glycosaminoglycans mediate the coacervation of human tropoelastin through dominant charge interactions involving lysine side chains. J. Biol. Chem. **274:**21719–21724.
56. **Yanagisawa, H., E. C. Davis, B. C. Starcher, T. Ouchi, M. Yanagisawa, J. A. Richardson, and E. N. Olson.** 2002. Fibulin-5 is an elastin-binding protein essential for elastic fibre development in vivo. Nature **415:**168–171.